

## Upward shifts in the southern Hydrate Ridge gas hydrate stability zone following postglacial warming, offshore Oregon

Nathan L. B. Bangs

University of Texas Institute for Geophysics, Austin, Texas, USA

Robert J. Musgrave

Department of Earth Sciences, La Trobe University, Bundoora, Victoria, Australia

Anne M. Tréhu

College of Oceanic and Atmospheric Sciences, Oregon State University, Corvallis, Oregon, USA

Received 2 July 2004; revised 8 November 2004; accepted 9 December 2004; published 26 March 2005.

[1] High-resolution three-dimensional (3-D) seismic reflection data acquired on the R/V *Thomas G. Thompson* in 2000 reveal a pair of bottom simulating reflections (BSRs) across a broad region of southern Hydrate Ridge, offshore Oregon. The primary BSR (BSR<sub>p</sub>) is a regionally extensive reflection that lies 120–150 m below seafloor and exhibits typical characteristics of a gas hydrate BSR. We also imaged a second weaker BSR (BSR<sub>s</sub>), 20–40 m below BSR<sub>p</sub>, with similar characteristics. BSR<sub>s</sub> is interpreted as a remnant of a BSR that probably formed during the Last Glacial Maximum 18,000 years ago, when the base of the gas hydrate stability zone (GHSZ) was deeper. An increase in bottom water temperatures of 1.75°–2.25° and a corresponding sea level rise of 120 m could have produced the BSR shift. The preservation of BSR<sub>s</sub> for at least 5000 years, which is the time since subseafloor temperatures stabilized following ocean warming after the Last Glacial Maximum, implies very slow upward advective and diffusive flow of methane (<1 m/1000 years in the vicinity of BSR<sub>s</sub>). BSR<sub>s</sub> appears where there are no resolvable steeply dipping faults and fractures, consistent with very low advective flow rates, and has dispersed where vertical fractures are visible. Free gas released by the shift in the BSR either migrates so slowly that it remains stable beneath the GHSZ or is directed upward along fractures to reform as hydrate in the GHSZ. There is no evidence for release of this free gas into the ocean or atmosphere.

**Citation:** Bangs, N. L. B., R. J. Musgrave, and A. M. Tréhu (2005), Upward shifts in the southern Hydrate Ridge gas hydrate stability zone following postglacial warming, offshore Oregon, *J. Geophys. Res.*, 110, B03102, doi:10.1029/2004JB003293.

### 1. Introduction

[2] BSRs (bottom simulating reflections) are distinctive, commonly observed seismic reflections that roughly parallel the seafloor. Although BSRs with positive polarity have been documented to form from mineral phase transitions such as opal CT to quartz [Hein *et al.*, 1978], most BSRs have clear negative polarity and are attributed to physical property contrasts generated by a sharp contact between gas hydrates above the BSR and a few percent free gas below it [Miller *et al.*, 1991]. Gas hydrate BSRs thus usually mark the base of the gas hydrate stability zone (GHSZ) defined by specific pressure and temperature (P-T) conditions.

[3] Geologic processes such as rising bottom water temperatures, sea level rise, and tectonic uplift shift sediment P-T conditions and hydrate stability zones. If global P-T changes cause an upward shift of the GHSZ, hydrate dissociation below the new GHSZ could potentially release

large volumes of methane stored in vast gas hydrate reservoirs around the world and affect global climate [Mienert *et al.*, 2000; Kennett *et al.*, 2003]. Recent observations of a rare, double BSR, in distinctively different, broadly ranging settings [Foucher *et al.*, 2002; Andreassen *et al.*, 2000; Mienert *et al.*, 2000] imply the possibility that shifting P-T conditions can leave behind a relict base of the gas hydrate stability zone [Foucher *et al.*, 2002]. These double BSRs may thus offer clues to the dynamics of hydrates by potentially revealing the response of gas hydrates to changing P-T conditions, and the potential for release of methane, which is a powerful greenhouse gas, into the ocean and atmosphere.

[4] In 2000, we acquired a high-resolution three-dimensional (3-D) seismic reflection data set across southern Hydrate Ridge to map the subsurface plumbing system and geophysical properties of the sediment related to the hydrate and free gas system. For the first time we image a double BSR with 3-D, high-resolution seismic data. This paper documents the regional extent and characteristics of a double BSR, and presents a qualitative model for its

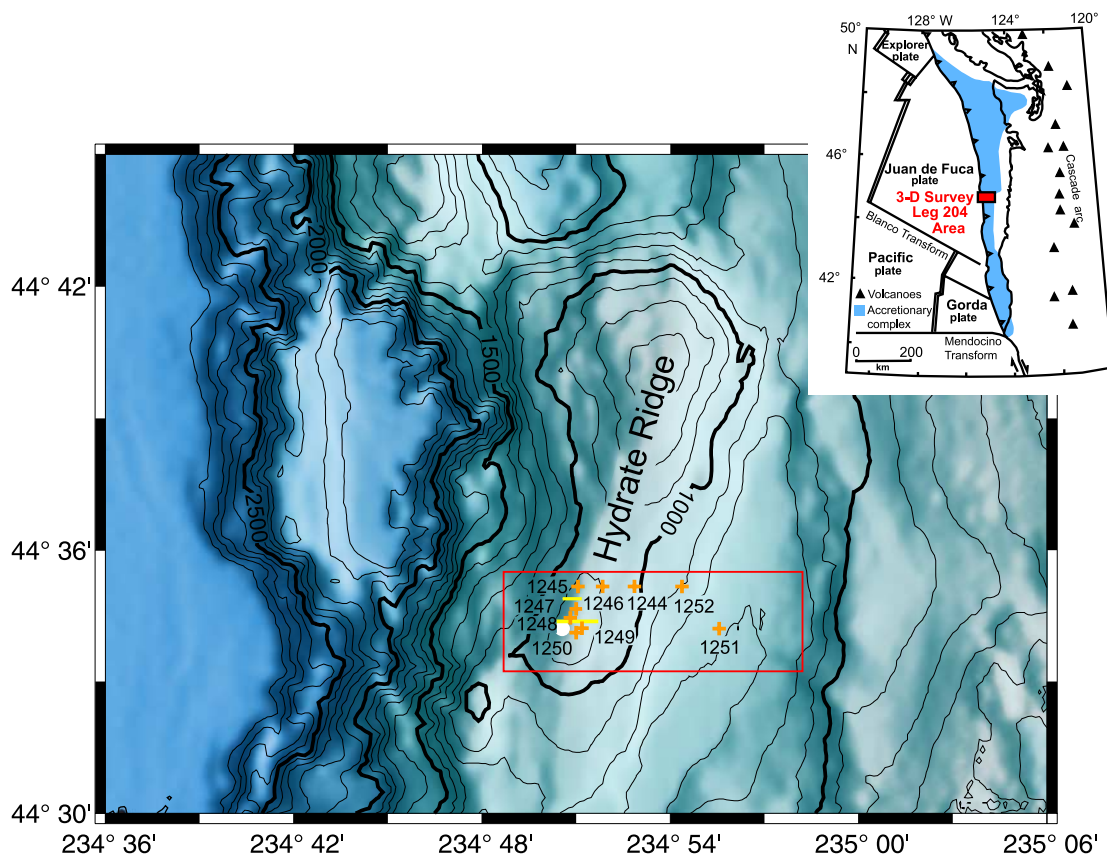


**Figure 1.** Location map showing 3-D area on southern Hydrate Ridge and the Leg 204 drill sites. Yellow lines mark the location of seismic line 296 shown in Figure 2a (southern line) and line 241 shown in Figure 12. White dot is the location of a 30 m high carbonate pinnacle protruding from the seafloor.

formation and evolution. We also present calculations estimating effects of these processes to first order in order to demonstrate the model's feasibility. Calculations are limited to first order because of a lack of constraint on past in situ conditions.

## 2. High-Resolution 3-D Seismic Reflection Data Acquisition and Processing

[5] The high-resolution 3-D seismic reflection data volume across southern Hydrate Ridge (Figure 1) served as a site survey for designing the drilling plan for Leg 204 [Tréhu *et al.*, 2003a] and for interpreting drilling results. Hydrate Ridge is a thrust ridge, uplifted by the collision between the subducting Farallon plate and the North American plate at a rate of  $\sim 4.5$  cm/yr in the Cascadia subduction zone. The crest of the ridge lies approximately 800 m below the sea surface, and forms a depositional basin on the landward (eastern) flank. The high-resolution 3-D seismic images of the ridge (Figure 2a) reveal detailed deformational structures, such as thrusting, tilting and folding of stratigraphic horizons.

[6] During the high-resolution 3-D seismic experiment we acquired 81 lines, each 11 km long, using a single streamer on the R/V *Thomas G. Thompson*. The lines are 50 m apart and thus cover a  $4 \times 11$  km<sup>2</sup> area (Figure 1). We used a Racal differential GPS (Global Positioning System) navigational system for determining ship's position and shot

spacing. For the seismic source we used two 0.65 L (40 in.<sup>3</sup>) Generator Injector (GI) guns, towed from floats 2.5 m below the sea surface, fired simultaneously at 15 m intervals. The GI guns are designed to provide a high-frequency (25–250 Hz) impulsive source with minimal bubble pulse interference. The source has a dominant frequency of 120 Hz and in these sediments ( $V_p < 1700$  m/s) the data resolve layers  $< 5$  m thickness. The receiver array was the Lamont portable high-resolution ITI solid-state streamer. It has 48 channels with 12.5 m receiver spacing for a total active array length of 600 m. Data were recorded at 1 ms sampling for 6 s. Streamer depth was maintained at 2.5 m using 5 control birds spaced every 150 m. The shallow depths were maintained in order to match the source tow depths and minimize receiver ghost effects at high frequencies. We reconstructed receiver positions from five compasses 150 m apart.

[7] The data were processed using Paradigm's Focus software. We edited noisy traces from shot gathers by inspecting each gather individually. The remaining traces were sorted into  $12.5 \times 25$  m bins with a nominal fold of 60 traces. Some extended binning was used to fill in low fold areas by replicating traces from adjacent bins. We applied normal moveout and stacked the binned traces following velocity analysis; however, these data are very insensitive to the velocity function because of the short maximum offset of  $\sim 600$  m. Data were migrated using 3-D poststack frequency-wave number time migration in Focus, which

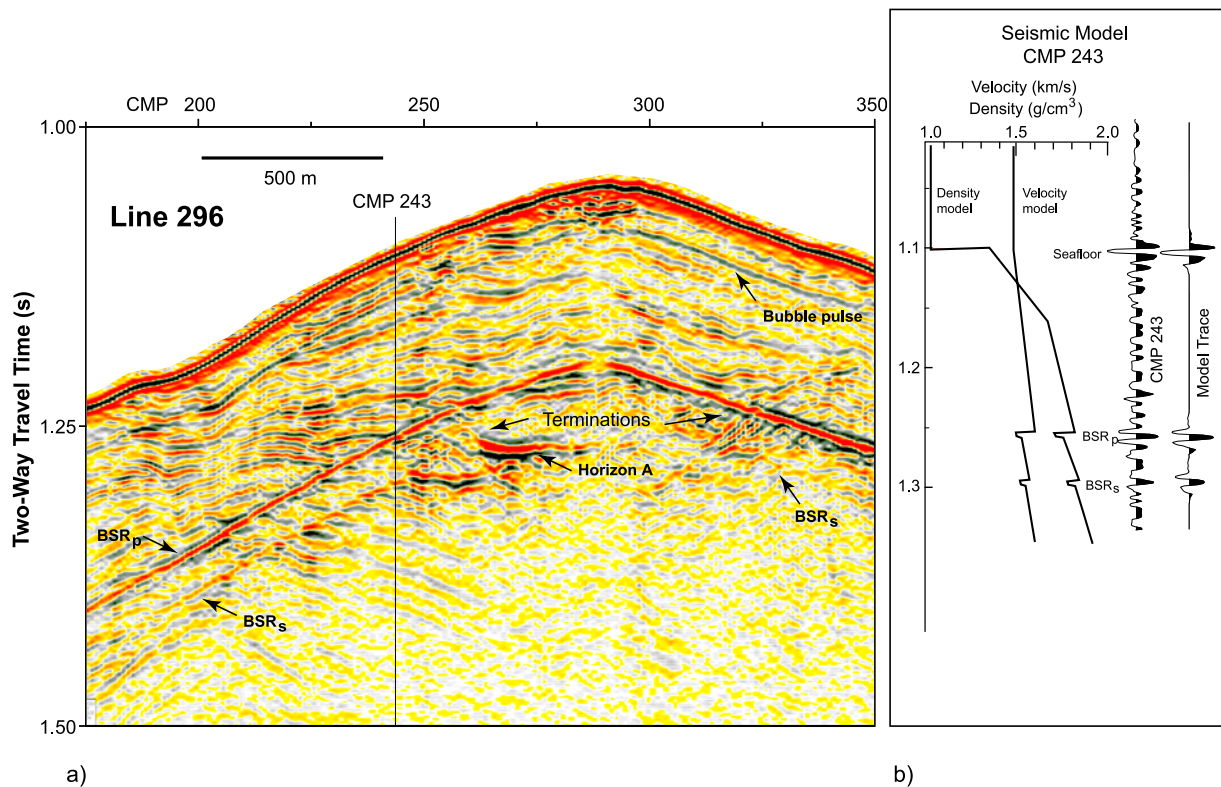


**Figure 2.** (a) A 1.5 km long portion of seismic line 296 across the crest of southern Hydrate Ridge from the 3-D seismic data volume. Display is true amplitude to compare relative amplitudes. Note BSR<sub>p</sub> is phase-reversed relative to the seafloor and intersects stratigraphic horizons closely paralleling the seafloor. BSR<sub>s</sub> lies 20–40 m below and is nearly parallel with BSR<sub>p</sub>. BSR<sub>s</sub> has the same phase as BSR<sub>p</sub> but is considerable weaker and discontinuous. Note the terminations and amplitude changes of stratigraphic horizons, especially horizon A, across BSR<sub>s</sub>. See Figure 1 for location. (b) Seismic model of CMP 243 from line 296 constructed to show velocity and density that could produce two BSRs. Thick lines are models that produce the model seismic trace on the right. Gradients are derived from Site 1247 log data. Seafloor reflection coefficient is estimated to be  $\sim 0.15$  by comparison with the seafloor multiple.

migrates reflections to their proper position in both inline and cross line directions.

### 3. BSRs Within Southern Hydrate Ridge

#### 3.1. Primary BSR

[8] BSRs are common throughout Hydrate Ridge and appear prominently in our 3-D seismic volume across southern Hydrate Ridge. A regionally extensive BSR stands out as a high-amplitude reflection that roughly parallels the seafloor across the crest of the ridge, 100–130 m beneath the seafloor (BSR<sub>p</sub> in Figure 2). On the true amplitude display in Figure 2a, the BSR is consistently one of the brightest subseafloor reflections. This reflection is readily distinguished as a gas hydrate bottom simulating reflection because it is phase reversed relative to the seafloor, roughly parallels the seafloor, and intersects dipping and deformed stratigraphic horizons. The reversed polarity indicates a decrease in seismic impedance (the product of velocity and density) and is consistent with the contrast between high-velocity sediments containing hydrate overlying low-velocity sediment containing free gas. The lowest velocities and low densities associated with BSR<sub>p</sub> are within a 5 m interval at the base of the GHSZ (Figure 2b).

#### 3.2. Second BSR

[9] Throughout areas of the 3-D data volume, predominantly on the western flank of the ridge, a second, relatively weak seismic reflection lies between 20 and 40 m below and nearly parallel to BSR<sub>p</sub> (Figure 2a). By comparison to BSR<sub>p</sub>, BSR<sub>s</sub> is considerably weaker and discontinuous. It is identifiable as a distinct reflection for about 500 m between common midpoint (CMP) 200 and CMP 250 in Figure 2a and fades into the noise level with only hints of the reflection across the rest of the profile. The polarity appears to be the same for both BSRs, suggesting that BSR<sub>s</sub> is also caused by a decrease in velocity and/or density across this interface. Figure 2b shows a model for the BSR<sub>p</sub> and BSR<sub>s</sub> at CMP 243 on line 296 showing that similar velocity and density changes and a low-velocity and low-density interval produce these reflections. CMP 243 was modeled because it has a locally high BSR<sub>s</sub> amplitude, which can be distinguished above noise and makes modeling easier.

#### 3.3. Correlation Between the BSRs

[10] BSR<sub>s</sub> is common throughout the 3-D data volume and nearly parallels the primary BSR (BSR<sub>p</sub>). In mapping the BSRs we have picked the largest amplitude lobe of the reflection (red in Figure 2a). The separation between the

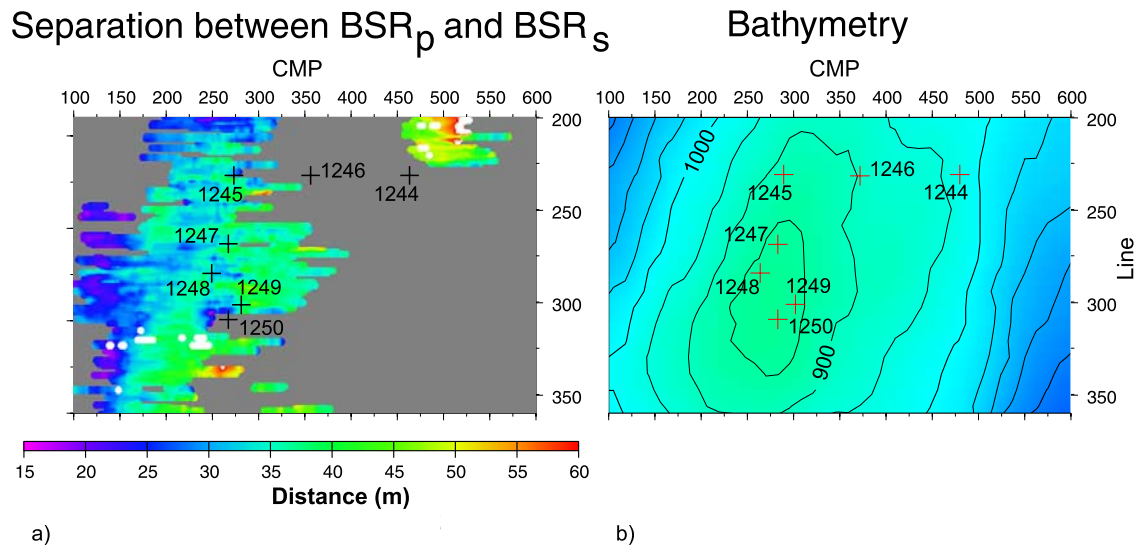


**Figure 3.** Maps showing (left) the thickness between  $BSR_s$  and  $BSR_p$  and (right) seafloor bathymetry in meters. These maps show a general relationship between the change in BSR depth and the seafloor bathymetry with exceptions.

BSRs varies from  $\sim 20$  m in the north and west to  $\sim 40$  m in the southern and eastern areas of its observed occurrence (Figure 3). We note that, with some exceptions, this variation corresponds approximately to the seafloor bathymetry (Figure 3, right), with greater separation beneath the ridge crest.

[11] The occurrence of  $BSR_s$  is very patchy; however, its occurrence is not random with respect to  $BSR_p$ . Figure 4 shows the region in which  $BSR_s$  occurs (outlined in red) and the areas of highest relative reflection amplitude (outlined in black).  $BSR_s$  amplitudes are 2–3 times less than  $BSR_p$  (Figure 4). The occurrence of  $BSR_s$  is distinctly located on the western flank of southern Hydrate Ridge, but, with a few exceptions, it lies beneath an area of moderate  $BSR_p$  amplitude and flanked by the areas of highest  $BSR_p$  reflection amplitudes (Figure 4b).  $BSR_s$  is not a bubble pulse or other artifact of the seismic wavelet, because if it were the amplitude of both BSRs would correlate well in amplitude and separation. They clearly do not.

[12] There is a bubble pulse that can be seen as a reflection that parallels the seafloor that is not a BSR. The bubble pulse is distinguishable by its consistent separation and amplitude correlation between the bubble and main source pulses. A reflection that parallels the seafloor (Figure 2a) has both of these attributes (Figure 5); however, the correlation is degraded in places by other reflections that interfere with the bubble pulse. Our examination of the BSRs recognizes and avoids the bubble pulse.

### 3.4. Reflection Amplitude Changes at the BSRs

[13] Reflection amplitudes of stratigraphic horizons are apparently altered by the transition into the GHSZ. Bright reflections below the BSR weaken or commonly terminate at the base of the primary BSR ( $BSR_p$ ) (e.g., on the eastern flank of Hydrate Ridge in Figure 2a), probably because of a change in the physical properties as free gas below the hydrate stability field changes to hydrate within the stability field. Where  $BSR_s$  is present, the reflection amplitudes of stratigraphic horizons are also consistently higher beneath

$BSR_s$  and appear to terminate or substantially decrease in amplitude across this deeper boundary. This is especially pronounced along horizon A (Figure 2a), which is a regionally extensive seismic reflection that we mapped from the northernmost line of the survey to the summit of southern Hydrate Ridge [Tréhu *et al.*, 2004b; Bangs *et al.*, 2001; Tréhu *et al.*, 2002, 2003a]. Where it was drilled on Leg 204, horizon A is usually a 2–4 m thick interval of fine sand turbidites containing abundant volcanic glass shards surrounded above and below by silty clays. Sandy turbidites presumably give it relatively high permeability. On the basis of Leg 204 density logs and other data, horizon A was interpreted as the primary conduit for free gas that has migrated from deep sources [Tréhu *et al.*, 2002, 2004b] and feeds free gas to the hydrate stability zone at the summit of southern Hydrate Ridge. The amplitude of horizon A should therefore be larger below the GHSZ than within it.

[14] A series of profiles across the western flank of southern Hydrate Ridge reveals a common relationship between BSRs and horizon A (Figure 6). Horizon A changes amplitude at both BSRs. Near the summit, the amplitude of horizon A decreases to near zero at  $BSR_s$ , and leaves little possibility for further decrease at  $BSR_p$ . Further north on lines 292 and 270, the amplitude decreases partially at  $BSR_s$ , and again at  $BSR_p$ .

## 4. Interpretation of the BSRs

### 4.1. Upper BSR ( $BSR_p$ )

[15] From Leg 204 evidence,  $BSR_p$  is a typical gas hydrate BSR that lies at the base of the GHSZ. The low velocities and densities that produce  $BSR_p$  lie within a  $\sim 5$  m thick layer that probably contains locally high concentrations of free gas. Observations of cores, infrared photographs of cores, pressure core samples, resistivity logs, and pore water geochemistry all indicate an abundance of hydrate above  $BSR_p$ , and none below it [Tréhu *et al.*, 2004a, 2003a]. Temperature profiles at Leg 204 drill sites predict the base of the gas hydrate stability field between

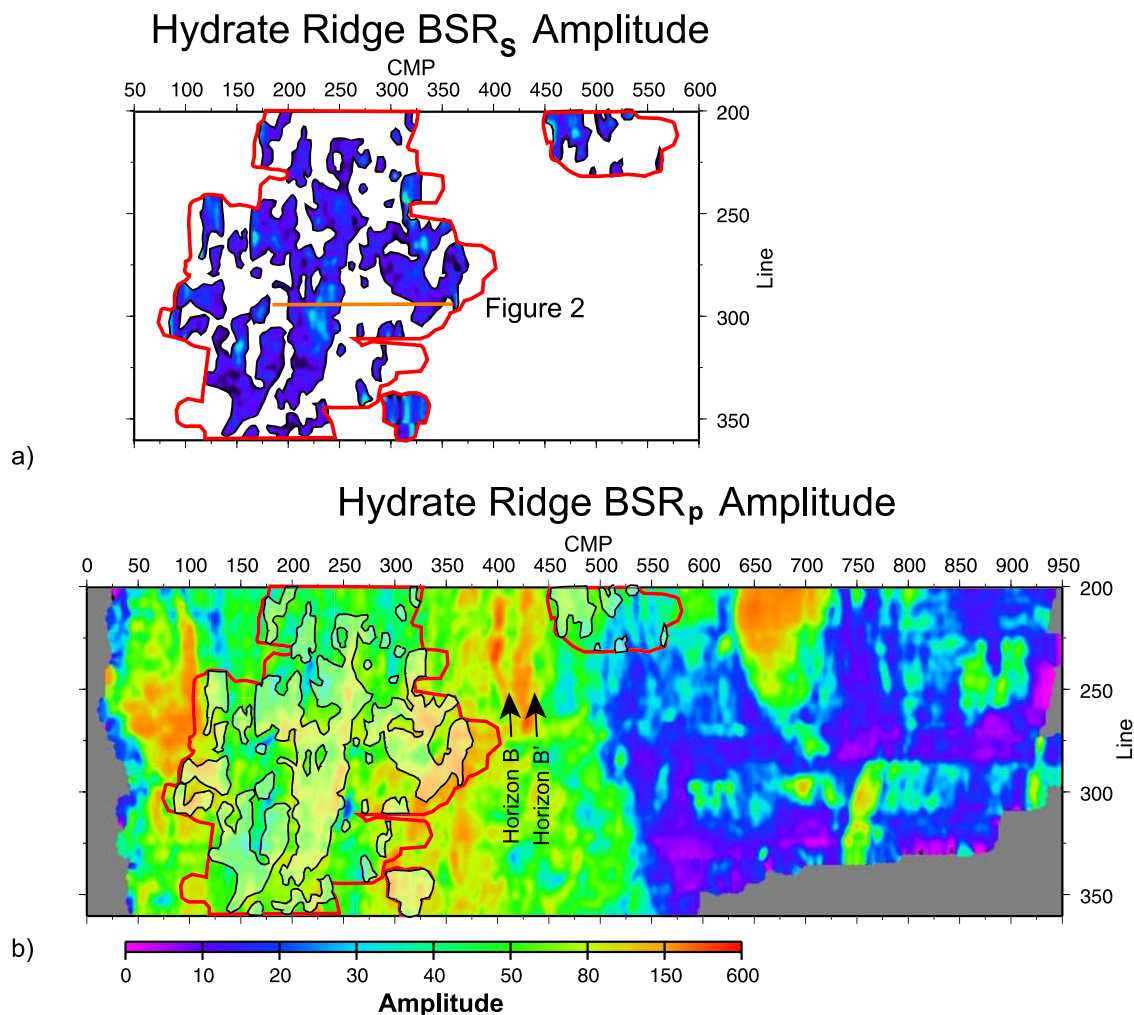


**Figure 4.** (a) Amplitude maps of  $BSR_s$ . Red outline shows the regional occurrence of  $BSR_s$ . Blue patchy areas show  $BSR_s$  where the amplitude is large enough to recognize the reflection. (b) Amplitude map of  $BSR_p$  with occurrence of  $BSR_s$  from Figure 4a superimposed. Note that  $BSR_s$  most commonly lies adjacent to the areas of highest  $BSR_p$  amplitude and beneath areas of moderate  $BSR_p$  amplitude. Arrows point to tuning effects on  $BSR$  amplitudes due to interference with other horizons (e.g., horizons B and B' described by Tréhu *et al.* [2003a], which are avoided in the interpretation of amplitudes.

$\pm 10$  and 20 m of the observed base of hydrate occurrence [Tréhu *et al.*, 2003a]. This places  $BSR_p$  at the predicted base of the methane hydrate stability field for structure I hydrates to within the limits of instrument errors. We interpret  $BSR_p$  as the active BSR in equilibrium with current P-T conditions that define the base of the hydrate stability field for structure I hydrates.

#### 4.2. Lower BSR ( $BSR_s$ )

[16] There are several possible interpretations for the deeper BSR,  $BSR_s$ . Our preferred interpretation is that  $BSR_s$  is a remnant from a time when the base of the gas hydrate stability was deeper in the section and subsequently shifted following changes in P-T conditions. However, we will first consider two other possibilities.

##### 4.2.1. Structure II Hydrate BSR

[17] Higher-order hydrocarbons, such as propane, lead to the formation of structure II hydrates [Sloan, 1997], which are stable at higher temperature than methane hydrate (structure I) and can therefore possibly form a second

BSR below the methane hydrate stability zone [Andreassen *et al.*, 2000]. Other gases, such as  $CO_2$  and  $H_2S$  have a similar effect on hydrate stability. The region between the two BSRs could contain free methane gas and structure II hydrate in the pore space. In that case, the depth of the second BSR should depend on the composition of gases present during formation of hydrates. Leg 204 drilling confirmed the presence of thermogenic hydrocarbons with locally high quantities of ethane, propane, and butane near  $BSR_p$ , especially in the vicinity of the primary gas conduit, horizon A [Tréhu *et al.*, 2003a], and  $BSR_s$  could be the base of the hydrate stability zone for structure II hydrates.

[18] Although we cannot completely rule out  $BSR_s$  as an effect of the presence of gases other than methane, several observations conflict with this interpretation. Most compelling, Leg 204 drilling found considerable evidence for hydrates above  $BSR_p$ , but no evidence was found for the presence of hydrates beneath  $BSR_p$ , either directly in cores, or indirectly as thermal anomalies in cores or resistivity anomalies in logs [Tréhu *et al.*, 2004a, 2003a]. Sites 1245,

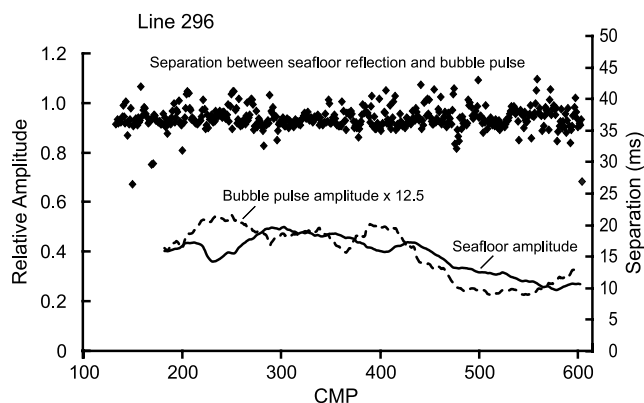


**Figure 5.** Characteristics of amplitude and separation relative to the seafloor reflection of the “bubble pulse” on line 296 (Figure 2a). Separation (diamonds) is consistently  $\sim 37$  ms and varies  $\sim 5$  ms. Amplitudes are smoothed with a 50-point running average. Amplitudes vary similarly; however, the bubble pulse is affected by interference from other reflections.

1247, 1248 and 1250 crossed both BSRs, offering several opportunities to observe the presence of hydrates between the BSRs, but we observed no hydrates or hydrate proxies.

#### 4.2.2. Opal/Quartz BSR

[19] Although rare compared to gas hydrate BSRs, silica phase transitions (opal-A to opal-CT or opal-CT to quartz) can also produce BSRs [Hein *et al.*, 1978; Kuramoto *et al.*, 1989]; however, they have geophysical signatures that are distinctive from a hydrate BSR. Because of a density increase across the opal-A to opal-CT transition these BSRs have normal reflection polarity, which is not observed in either  $BSR_s$  or  $BSR_p$  in our data. Furthermore, temperature is a critical factor for these mineral phase transitions. Opal-A/opal-CT BSRs were found at temperatures between  $35^\circ$  and  $50^\circ\text{C}$  in Leg 127/128 in the Sea of Japan [Kuramoto *et al.*, 1989], and the opal-CT to quartz transition was found at temperatures above  $50^\circ\text{C}$  at Site 1173 in the Nankai Trough [Mikada *et al.*, 2002]. Leg 204 temperature measurements at the BSR were substantially lower; typically  $\sim 10^\circ\text{C}$ . Neither of the BSRs within Hydrate Ridge can therefore be attributed to silica phase transitions.

#### 4.2.3. Relict BSR

[20] Changes in pressure and temperature in sediments will shift the GHSZ (Figure 7) and disrupt the BSR.  $BSR_s$  could be a remnant of an older gas hydrate stability boundary that is in the process of dispersing, as others have predicted [e.g., von Huene and Pecher, 1999; Pecher *et al.*, 2000] and interpreted [e.g., Foucher *et al.*, 2002] elsewhere. The polarity and seismic models of  $BSR_s$  (Figure 2b) are consistent with a thin layer of free gas that is typical of a BSR that forms along the base of the gas hydrate stability zone. If the current BSR ( $BSR_p$ ) is representative of the continuity of an active BSR,  $BSR_s$  has developed a patchiness and weak reflection amplitude, probably from variable amounts of dispersion of the gas comprising  $BSR_s$  by fluid advection or methane diffusion since the shift from  $BSR_s$  to  $BSR_p$ .

[21] In addition to the double BSRs, there is evidence from other seismic reflections that support an upward shift

in the hydrate stability zone. As noted above, strong reflection amplitudes of dipping stratigraphic horizons usually extend up to  $BSR_p$  but decrease abruptly across it. We interpret the locally high amplitude of horizon A to be due to the presence of free gas beneath the BSR. Free gas is known to significantly affect reflectivity because of the effects of free gas on P wave velocity [Domenico, 1976]. The change in reflection amplitude is likely a result of the transition from free gas within the sediments below the hydrate stability

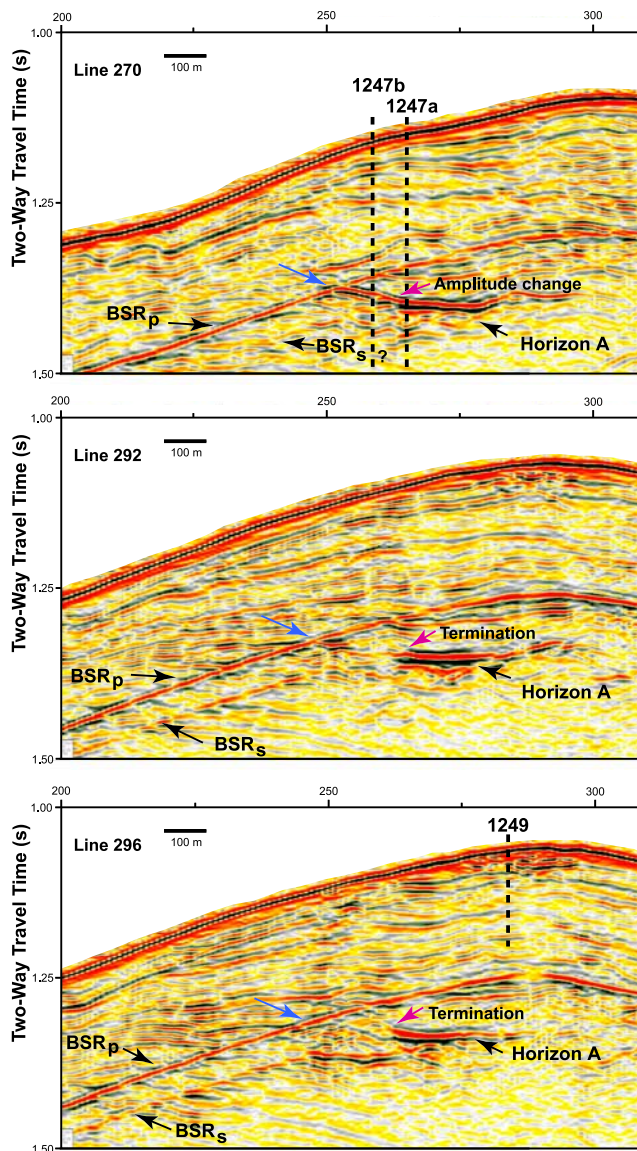


**Figure 6.** Three parallel seismic sections across the crest of southern Hydrate Ridge between Sites 1249 and 1247. Displays are true amplitude to show the relative amplitude of reflections in each of the profiles. Note the progression from the relatively high amplitude of  $BSR_s$  in line 296 to low amplitude of  $BSR_s$  in line 270. Purple arrows mark the coincident progression from the abrupt termination of horizon A at  $BSR_s$  in line 296 to continuous reflections across  $BSR_s$  in line 270. Blue arrows show a coincident increase in reflection amplitude at the intersection of horizon A and  $BSR_p$ .

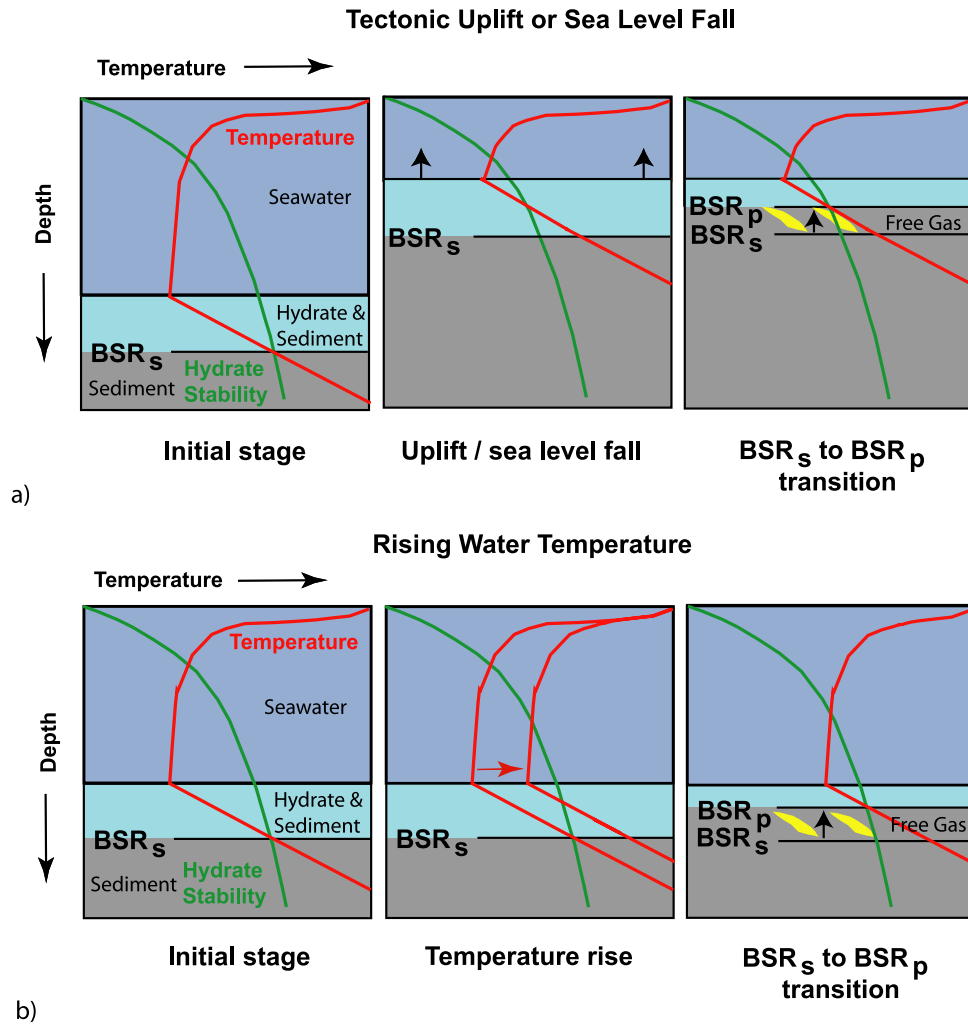


**Figure 7.** Cartoons showing two mechanisms for creating a double BSR. (a)  $BSR_s$  at the initial equilibrium stage lies at the intersection of the temperature (red line) and hydrate stability (green line) profiles. Tectonic uplift or sea level fall reduces overburden pressure and shift sediments relative to the hydrate stability curve and shifts the temperature profile. The  $BSR_s$  shifts to  $BSR_p$ , releasing free gas into sediments (yellow areas) from hydrate dissociation. (b) Bottom water temperature rising and conducting into the sediments, increasing sediment temperatures while maintaining the thermal gradient. Elevated temperatures shift the hydrate stability boundary upward.  $BSR_s$  shifts to  $BSR_p$ .

zone to gas hydrate above it. However, where  $BSR_s$  is observed, the amplitude change is often below the base of the GSHZ at  $BSR_s$  rather than at  $BSR_p$ . There are some relatively high-amplitude reflections from horizon A between the BSRs as noted in Figure 6 (blue arrows). Therefore there is probably some free gas beneath  $BSR_p$ , but the terminations of horizon A at  $BSR_s$  suggest that free gas that accumulated at the old BSR ( $BSR_s$ ) is still there and may be in the process of migrating up to the new BSR ( $BSR_p$ ). This interpretation is consistent with a transition of the hydrate stability field from  $BSR_s$  to  $BSR_p$  and inconsistent with other alternatives such as structure II hydrates.

## 5. Discussion

[22] The evidence presented here supports the existence of two BSRs as due to a shift in the BSR from  $BSR_s$  to  $BSR_p$  as a response to changes in P-T conditions. However, several puzzling questions remain about observing two

BSRs. What caused the shift in the BSR, and is it geologically reasonable and consistent with the recent conditions within southern Hydrate Ridge? When did the upward shift happen and how old is the relict BSR? What does the double BSR imply about the dynamics of hydrates, the BSR, and migration of free gas through the sediments and into the ocean or atmosphere after release from hydrate dissociation following the P-T shift (i.e., the clathrate gun hypothesis)?

[23] A likely geologic cause for the BSR shift is changing P-T conditions following warming since the Last Glacial Maximum. *Waelbroeck et al.* [2002] estimate that bottom water temperatures have risen by 2.2°C and that sea level has risen 120 m since the Last Glacial Maximum, 18,000 years ago (Figure 8). Both changes would have had a substantial effect on the position of the BSR. Sea level rise and bottom water temperature changes since the Last Glacial Maximum, however, should have had a global effect on hydrate stability, yet

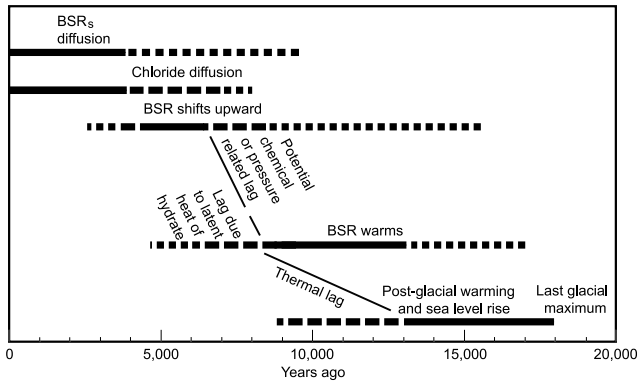


**Figure 8.** Timeline to illustrate the timing of various events and processes that led to the development of BSR<sub>s</sub>. Solid lines are likely timing and duration of events. Dashed lines represent the likely uncertainty. Diagonal lines are various time lags that may have delayed the upward shift of BSR<sub>s</sub>. See text for more details.

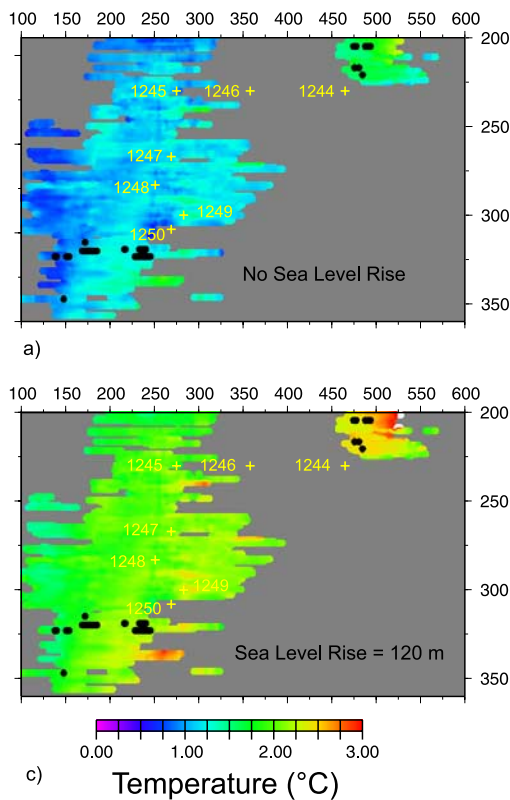
observations of a double BSR are relatively rare. We will first consider the possibility of localized changes in P-T conditions within Hydrate Ridge as the cause of the shift in the BSR before examining if BSR<sub>s</sub> could be a relict BSR from the Last Glacial Maximum.

### 5.1. Tectonic Uplift, Sea Level Fall, or Temperature Rise?

[24] We calculated the magnitude of tectonic, sea level or thermal effects for a 20–40 m upward shift of the BSR to examine whether these effects are geologically reasonable for Hydrate Ridge. Figure 7 shows the effects on the GHSZ from either a pressure decrease from tectonic uplift (or sea level drop), or an increase in bottom water temperature. Although at equilibrium there is an identical outcome from either of these scenarios, bottom temperature changes, unlike pressure effects, have significant time lags due to thermal propagation from the seafloor to the BSR. We assume that temperature equilibrates to a constant thermal gradient or a constant basement temperature at 6 km depth [Tréhu *et al.*, 1994], which are within error limits of each other (55°C/km versus 54.6°C/km, respectively).

[25] Figure 9 shows the amount of tectonic uplift (or sea level fall) or of bottom water temperature increase needed to explain the observations. In each of the maps we use the hydrate stability curve of Dickens and Quinby-Hunt [1994] for hydrate formation in the presence of seawater. On the basis of the observed thermal gradients of 53–57°C/km at Leg 204 drill sites, we assumed a constant thermal gradient of 55°C/km [Tréhu *et al.*, 2003a]. Following the scenario depicted in Figure 7a, we calculate an uplift (or sea level fall) of 100–170 m to shift the BSR from BSR<sub>s</sub> to BSR<sub>p</sub> (Figure 9a). (A second-order effect is the effect of a bottom

#### Bottom Water Temperature Change



#### Tectonic Uplift or Sea Level Fall

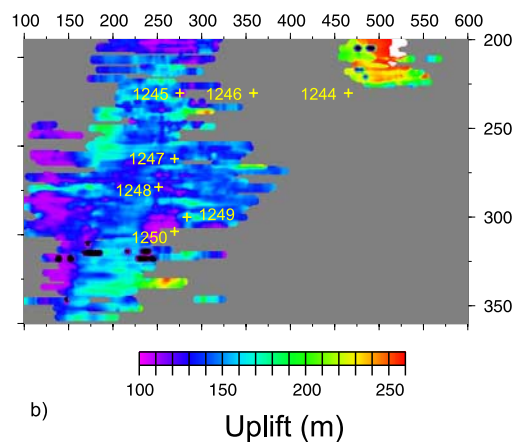


**Figure 9.** Maps of bottom water temperature changes and/or tectonic uplift required to match observed shift from BSR<sub>s</sub> to BSR<sub>p</sub>. (a) Bottom water temperature changes only, (b) tectonic uplift (or sea level fall) only, and (c) bottom water temperature changes assuming simultaneous 120 m sea level rise.



water temperature change associated with a change in the water column height. Estimates from current seawater temperature profiles [Tréhu *et al.*, 2003a] are 0.20/100°C. After this temperature change propagates to the BSR, it will affect BSR depth by ~25%. For simplicity, it will be ignored in this discussion.) The greatest uplift occurs near the crest of Hydrate Ridge. Following the scenario depicted in Figure 7b, the rise in bottom water temperatures needed to shift the BSR from BSR<sub>s</sub> to BSR<sub>p</sub> is 0.75°–1.25° (Figure 9b).

[26] Is tectonic uplift a reasonable cause of the shift of the BSR in southern Hydrate Ridge? This question can be addressed by determining if 100–170 m of uplift could occur within a short enough time for BSR<sub>s</sub> to survive the diffusion and advective processes that will disperse it. It has taken ~1.6 my to raise trench sediments of this age from a depth of ~2,900 m to their present depth of ~1000 m. The long-term average uplift rate is 0.001188 m/yr. It would therefore take 85,000–143,000 years (63,000–108,000 years with the 25% correction) on average to uplift the ridge 100–170 m. Foucher *et al.* [2002] estimate roughly that the free gas layer that produces the relict BSR cannot survive more than ~10,000 years without dispersing by diffusion or advection (discussed further below).

[27] Recent uplift might be substantially faster than the average uplift rate if recent uplift occurred from an extreme tectonic event, such as seamount or ridge subduction. In the extreme case, all of the plate convergence might occur along faults beneath Hydrate Ridge and an uplift of 100–170 m could be possible in 4400–7400 years. However, there is no evidence that such an extreme event is currently underway, so we conclude that tectonic uplift can be ruled out.

[28] Furthermore, the transition from BSR<sub>s</sub> to BSR<sub>p</sub> probably represents two periods of relatively stable P-T conditions separated by a period of rapid changes. Uplift of 100–170 m would probably have to occur in multiple stages that would generate additional BSRs in between BSR<sub>s</sub> and BSR<sub>p</sub>, and these are not seen.

[29] Could local bottom water temperature changes cause a shift in the BSR? Figure 9 shows that a temperature increase of 0.75–1.25°C would cause the observed BSR shift. The larger temperature shifts are associated with shallower seafloor depths, which is reasonable from downward propagation of surface water warming in recent times. However, if bottom water warming does not occur on the timescale of <5000 years, global bottom water temperatures and sea level rise since the Last Glacial Maximum will also affect the hydrate stability boundary. Local bottom water temperature changes on Hydrate Ridge can be considered a possibility if they occurred recently enough to be distinct from global glacial events. There is a considerable time lag associated with the propagation of bottom water temperatures through the sediments to the depths of the BSR. Figure 10 shows temperature profiles to depths of the BSR following an increase in bottom water temperature of 2° following Loudon and Wright [1989]. Thermal lags initially affect the BSR little, and then a rapid upward shift is followed by a slow rise to equilibrium. Observed temperature profiles from Leg 204 are consistent with an equilibrium conductive thermal gradient and show no indication of a downward propagating thermal pulse. On the basis of the observation that the upward position of the BSR does not begin to stabilize until 5000 to 10,000 years after the initial

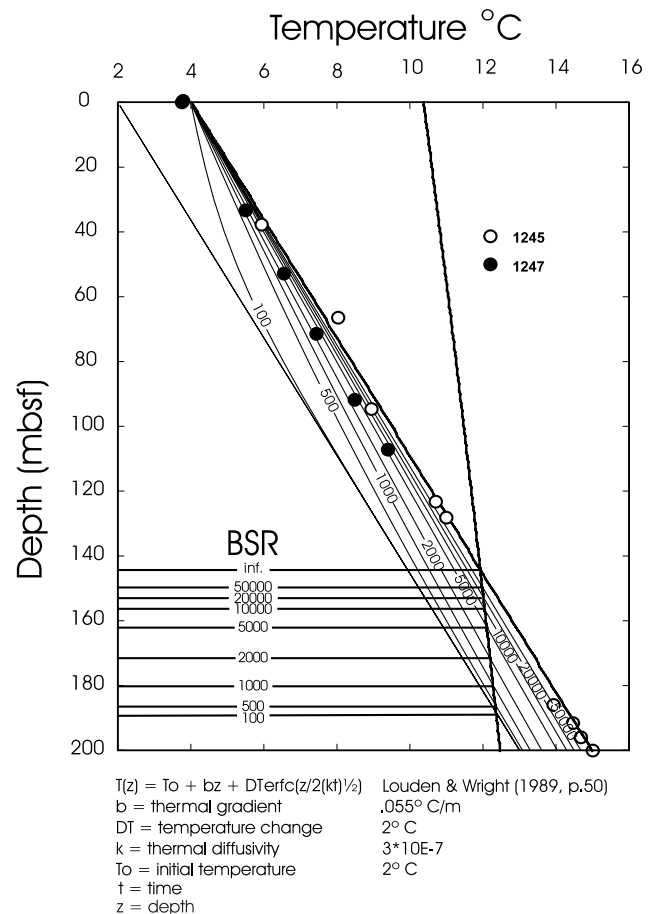


**Figure 10.** Temperature data for Sites 1245 (open circles) and 1247 (solid circles) and calculated temperature profiles (thin annotated curves) following a bottom water temperature increase from 2° to 4°. We assume a temperature gradient of 0.055°/m, which fits data from Site 1245 well, and may be slightly high for Site 1247. Numbers indicate years following temperature change. Thick line on the right-hand side is the theoretical base of the gas hydrate stability zone for hydrate in seawater [Dickens and Quinby-Hunt, 1994]. Horizontal lines are the positions of the BSR at various times. Note that the BSR does not become stable for at least 5000 years and possibly 10,000 years. Temperature data suggest a bottom water temperature rise of 2°C would have had to occur at least 5000 years ago and possibly 10,000 years ago.

pulse, we speculate that bottom water temperature changes large enough to shift the BSR significantly had to occur more than 5000 and possibly as much as 10,000 years ago (Figure 8).

## 5.2. BSR<sub>s</sub>, a Remnant From the Last Glacial Maximum

[30] A shift in the BSR is likely the result of postglaciation P-T changes within Hydrate Ridge as suggest by others for northern Cascadia [Westbrook *et al.*, 1994], southwestern Japan [Foucher *et al.*, 2002], and the Norwegian margin [Posewang and Mienert, 1999]. Estimates of bottom water temperatures from <sup>18</sup>O isotopes taken from benthic forams in the Pacific show a 2.2° rise in temperatures in the past 18,000 years [Waelbroeck *et al.*, 2002]. The largest in-

crease occurred between 10,000 and 18,000 years ago. Concurrently, *Waelbroeck et al.* [2002] estimate that sea level has risen globally by 120–130 m. While a bottom water temperature rise of  $2.2^\circ$  is substantially larger than what is needed to shift BSR<sub>s</sub> to BSR<sub>p</sub>, the sea level rise has an opposite effect on the position of the base of the hydrate stability zone. Figure 9c shows changes of  $1.75$ – $2.25^\circ$  will shift BSR<sub>s</sub> to BSR<sub>p</sub> with a coincident 120 m sea level rise. These changes in bottom water temperatures and sea level since the Last Glacial Maximum, most of which occurred more than 10,000 years ago, are sufficient to cause a shift of the BSR from BSR<sub>s</sub> to BSR<sub>p</sub>. Given the lag in thermal propagation, we believe that the observed changes in bottom water temperatures and sea level rise that have occurred since the Last Glacial Maximum are a better explanation of the shift of the BSR than a smaller, more recent bottom water temperature change (Figure 8).

### 5.3. Time Frame for the BSR Shift

[31] The time frame of the BSR shift is further critical evidence that BSR<sub>s</sub> shifted as part of the last glacial cycle, but also it reveals the dynamics of the hydrate/free gas system in response to the changing P-T conditions. The observation of a relict BSR, puts constraints on the time-scale over which gas hydrates decompose and the products of this decomposition disperse in nature. If concentrations of free gas within the BSR<sub>s</sub> layer (Figure 2b) are below the threshold for percolation, which they likely are, the mechanism for methane migration is diffusion within the pore fluid or advection with migrating pore fluids [*Henry et al.*, 1999]. Temperature profiles measured on Leg 204 show linear thermal gradients to within the limitations of the instrument error (Figure 10). We estimate from the temperature profiles at Sites 1245 and 1247 that upward advection can not be greater than  $3.5 \times 10^{-10}$  m/s or 11 m/1000 years and still fit the temperature profile. The advection model follows *Turcotte and Schubert* [1982, p. 401] and assumes thermal conductivity of 1.0 W/m °K, fluid density of 1000 kg/m<sup>3</sup>, fluid specific heat of 4000 J/kg °K, and a reservoir temperature of 50°C. At this advection rate BSR<sub>s</sub> would disperse half the seismic wavelength ( $\sim 10$  m) in 900 years. We speculate that BSR<sub>s</sub> would not be recognizable in the seismic section unless advection has been extremely slow, substantially less than 11 m/1000 years.

[32] In an alternative scenario, *Foucher et al.* [2002] make a crude estimate that without any advection, or free gas percolation, a free gas interval would diffuse 10 m, more than enough to become seismically unrecognizable, in 1000 years. Following *Foucher et al.* [2002], a rough estimate of the average diffusion distance can be made for Hydrate Ridge. Methane concentration measurements [*Milkov et al.*, 2003] indicate some undersaturated samples between the free gas intervals that produce the BSRs, and therefore there is a concentration gradient that can drive diffusion. If we assume a linear concentration gradient, we can use the Einstein-Smoluchowski equation [*Levine*, 1978] for diffusion ( $x_{\text{rms}} = (2Dt)^{1/2}$ ) where  $x$  is the diffusion distance,  $D$  is the diffusion coefficient, and  $t$  is time. If we conservatively assume the same value for  $D$  (0.02 m<sup>2</sup>/yr) as *Foucher et al.* [2002] ( $D$  depends on temperature, porosity, and tortuosity but should range between 0.021 and 0.023 m<sup>2</sup>/yr for sediments between 0 and 500 m below

seafloor [*Martin et al.*, 1996]) and that the BSR free gas layer diffuses both upward and downward an average of 5 m (10 m total), the estimated time is 625 years (*Foucher et al.* [2002] estimate this as  $\sim 1000$  years). *Foucher et al.* [2002] also assume that with the presence of free gas, which dissolves into solution as methane diffuses away, the diffusion time increases in proportion to the ratio of total methane to dissolved methane, which they estimate as 3–10 from pressure core sampler (PCS) measurements from Blake Ridge. On the basis of a few Leg 204 PCS measurements between the BSRs it is  $\sim 3$  [*Milkov et al.*, 2003] but probably higher at BSR<sub>s</sub> (Figure 2b). *Foucher et al.* [2002] estimate diffusion would disperse a BSR 10 m in  $<10,000$  years. A similar rough estimate of diffusion of a BSR layer 10 m for Hydrate Ridge could also be 3000–10,000 years (Figure 8). Preservation of a BSR long enough to survive since postglacial warming is probably only possible with near-zero fluid advection and high enough free gas concentrations within BSR<sub>s</sub> to assure that it does not diffuse away quickly. Low velocities and densities below BSR<sub>s</sub> is evidence for the free gas that could help sustain BSR<sub>s</sub> (Figure 2b) [*Tréhu et al.*, 2003a].

[33] Further critical evidence for the age of BSR<sub>s</sub> is possible by comparing observed chloride measurements in pore fluids between the BSRs acquired during Leg 204 drilling with models of Cl<sup>-</sup> anomaly diffusion. Figure 11 shows Cl<sup>-</sup> data from Site 1247 in the vicinity of the BSRs. Superimposed are models of Cl<sup>-</sup> anomaly diffusion constructed following *Ussler and Paull* [2001] for various periods after hydrate dissociation. We assume that the Cl<sup>-</sup> anomaly produced immediately after hydrate dissociation resembles that observed above the current BSR (BSR<sub>p</sub>) at Site 1247 in its magnitude (40 mM) and width (10 m) (Figure 11), which is consistent with  $\sim 8\%$  hydrate saturation [*Tréhu et al.*, 2004a]. A reasonably good model of diffusion of such a Cl<sup>-</sup> anomaly is that produced after  $\sim 5000$  years. The model implies a time range for methane dissociation of between  $\sim 4000$  and 8000 years ago. This result suggests that the BSR probably shifted  $\sim 5000$  years ago (Figure 8).

[34] We have argued that from the chloride anomaly that the BSR shift occurred 4000–8000 years ago, which is reasonable given that the longevity of a relict BSR could be as much as 10,000 years. However, can BSR<sub>s</sub> be due to known bottom water temperature changes that began at the Last Glacial Maximum 18,000 years ago? The thermal propagation lag of  $\sim 5000$  years is a significant lag that improves the timing between the postglacial warming and the BSR shift, it may also be that the thermal lag is longer (up to 10,000 years, Figure 10), but there may be additional delays in the shift of the hydrate stability boundary following the rise in bottom water temperature. One possibility is a lag due to latent heat needed to dissociate the hydrate. We estimate that small quantities of  $\sim 6\%$  hydrate (10% of pore space with 60% porosity) within the 40 m between the BSRs requires dissociation of 2160 kg of hydrate per square meter. This amount requires  $8.8 \times 10^9$  J of heat (latent heat of  $-407$  kJ/kg [*Ruppel*, 1997]), which could be produced in just 500 years with a heat flow of 0.55 J/m<sup>2</sup> (assuming a thermal gradient of 0.055°C/m and thermal conductivity of 1.0 W/m °C [*Tréhu et al.*, 2003a] (Figure 8). Elevated pore fluid pressures following hydrate dissociation could inhibit

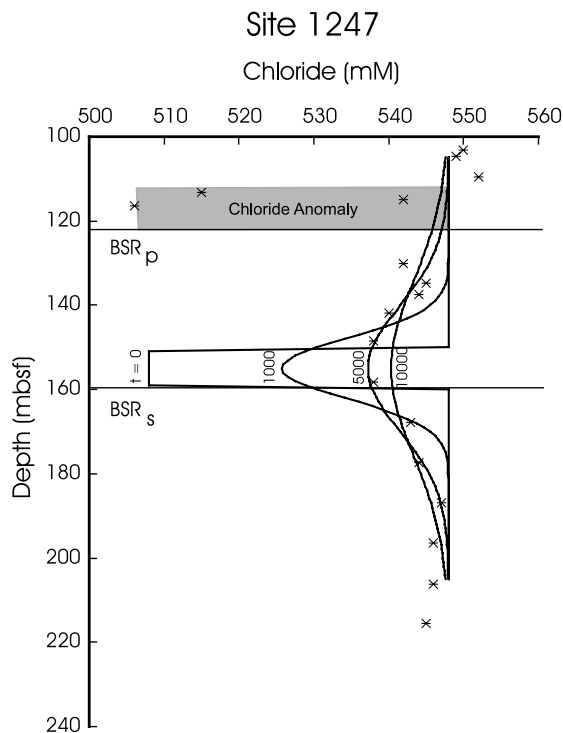


**Figure 11.** Chloride concentrations in pore water samples from Site 1247 compared with expected  $\text{Cl}^-$  concentrations derived from a model of a  $\text{Cl}^-$  diffusion following hydrate dissociation. Crosses are Site 1247  $\text{Cl}^-$  pore water data. Note the freshening above  $\text{BSR}_p$ , which is attributed to hydrate dissociation. The initial model,  $t = 0$ , has width (10 m) and magnitude comparable to the  $\text{Cl}^-$  anomaly above  $\text{BSR}_p$ . Hydrate diffusion is calculated following *Ussler and Paull* [2001] using diffusion equation 2.15 from *Crank* [1975]. We used a diffusion coefficient of  $2.5 \times 10^{-9} \text{ m}^2/\text{s}$ . The data are reasonably well matched at  $t = 5000$  years. The age of  $\text{BSR}_s$  is probably  $<8000$  years and  $>4000$  years.

the upward migration of the hydrate stability field and the BSR by compensating for the temperature rise and effectively delay the shift of the BSR [*Pecher et al.*, 2000]. However, we can only speculate on past fluid pressures. Pore water freshening effects following hydrate dissociation would change the P-T phase boundary for free gas and gas hydrate in pore fluid [*Dickens and Quinby-Hunt*, 1994], which would also stabilize the BSR during a temperature rise. The effect, however, could only be sustained for a significant time with slow advection and diffusion of freshened pore waters. These additional mechanisms can potentially contributed to delay the shift of the BSR and improve the timing between the known bottom water warming and the BSR shift (Figure 8).

#### 5.4. Dynamics of Gas Hydrate, BSRs, and Free Gas

[35] If our interpretation of the double BSR as an upward shift from  $\text{BSR}_s$  to  $\text{BSR}_p$  following postglacial maximum warming is correct, then the changes in P-T conditions implied by the double BSR have created a natural experiment for examining the effects of changing P-T condition on the BSR, gas hydrates and the free gas system. *Kennett et al.* [2003] describe release of methane during interglacial

periods following bottom water warming as the “clathrate gun hypothesis.” The results presented here examine just such a scenario.

[36] As discussed above, preservation of the BSR for 5000 years implies extremely slow upward advective flow and high gas concentrations at  $\text{BSR}_s$ . We suggest that areas where  $\text{BSR}_s$  is preserved have a lower advective flow rate than the areas where  $\text{BSR}_s$  is not observed. Fracture permeability from faults probably has a large role in preservation of  $\text{BSR}_s$ . Figure 12 shows the disappearance of  $\text{BSR}_s$  where normal faults developed from uplift and extension of the crest of southern Hydrate Ridge. These normal faults are typically found on the eastern flank of southern Hydrate Ridge coincident with both a weak or nonexistent  $\text{BSR}_s$  and higher  $\text{BSR}_p$  amplitudes.

[37] This observation has two implications.

[38] 1. The formation of  $\text{BSR}_p$  above a relict  $\text{BSR}_s$  occurs even without upward migration of free gas. If upward migration of gas were required to develop  $\text{BSR}_p$ , it would simultaneously destroy the relict  $\text{BSR}_s$ . Where  $\text{BSR}_s$  has dispersed, advective flow may have also enhanced the gas concentration and contributed to enhance the  $\text{BSR}_p$  seismic reflection amplitude.  $\text{BSR}_p$  amplitude is higher in areas where  $\text{BSR}_s$  is not preserved. However, a relatively strong  $\text{BSR}_p$  still forms above  $\text{BSR}_s$  even though very little advective or diffusive migration of free gas has occurred, as the survival of  $\text{BSR}_s$  implies.  $\text{BSR}_p$  must therefore form from exsolution from fluids saturated or supersaturated in methane.

[39] 2. Localized fractures probably control the migration of free gas released from hydrate dissociation following a major warming event like the recent postglacial warming. Gas migration along fractures can also serve to direct free gas from beneath the hydrate stability zone into it, as also inferred in the Blake Ridge [*Gorman et al.*, 2002]. *Tréhu et al.* [2004a] noted higher concentrations of hydrates within and near vertical fractures on the eastern flank of Hydrate Ridge at Sites 1244 and 1246, relative to the western flank at Site 1245 where there are fewer vertical fractures. We do not see indications that the BSR is perturbed upward at faults due to upward advection of warm fluids along these faults. *Tréhu et al.* [2003b] calculate that a minimum flow rate of  $>1 \text{ cm/yr}$  is needed to observe such a perturbed BSR, while an upward advection rate of  $>1 \text{ cm/yr}$  would dissipate  $\text{BSR}_s$  in  $<1000$  years.

#### 5.5. Significance of the Double BSR

[40] While rising bottom water temperatures following the Last Glacial Maximum are a global phenomenon, the occurrence of two parallel BSRs is a relatively rare observation and is thus an indicator of global and local conditions. These conditions are likely (1) a lengthy period of stable P-T conditions that established a significant BSR initially, (2) a significant shift in P-T conditions, (3) little or no fluid advection following a shift in P-T conditions, and (4) sufficient free gas to prevent BSRs from dispersing quickly by diffusion. The observation of a double BSR thus implies that there is unusually high methane concentration in pore waters, some probably released from hydrate dissociation following the shift in bottom water temperatures as described in the “clathrate gun hypothesis” [*Kennett et al.*, 2003]. However, the clathrate gun hypothesis does not work

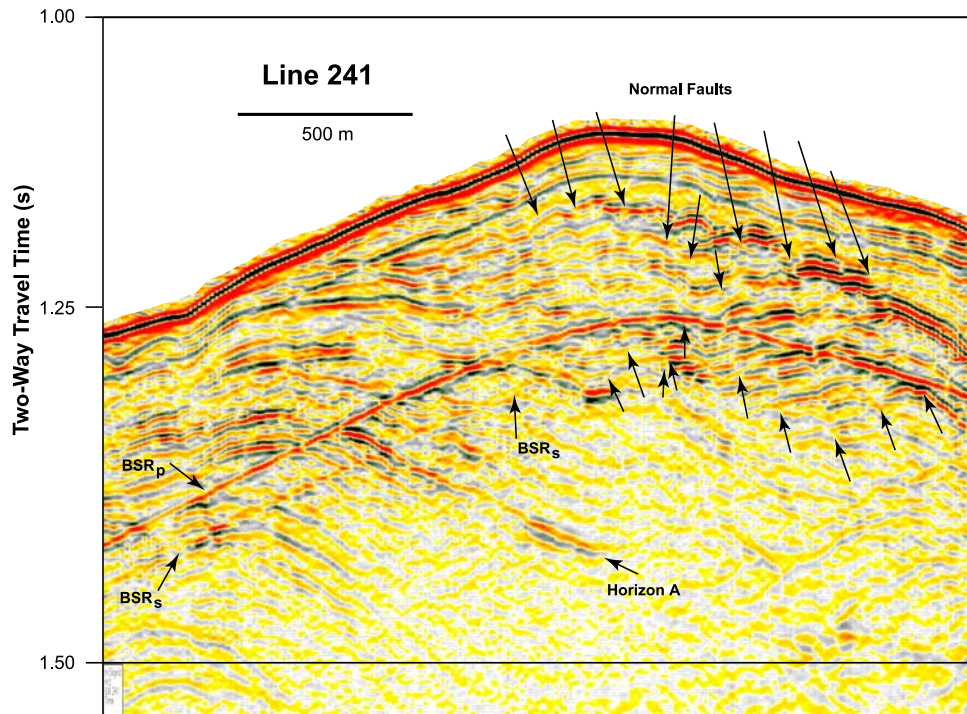


**Figure 12.** Seismic line 241 showing a coincident relationship between the amplitude of  $BSR_s$  and the location of numerous normal faults (between arrows). This is a true amplitude display. See Figure 1 for location. See text for details.

here, because once released, the free gas migrated very little and was not released into the atmosphere. Although the double BSR is rare, it may be rare because of unusually high free gas concentrations within the relict BSR as much as it is due to slow methane migration. Areas without a double BSR may also be areas of slow upward migration of methane that would impede release of methane into the atmosphere described in the “clathrate gun hypothesis”. Areas of southern Hydrate Ridge where  $BSR_s$  is not preserved have vertical faults and fractures that have increased the advective flow enough to disperse  $BSR_s$ , but have also directed the gas upward into the hydrate stability zone where it has reformed as gas hydrate and enhanced local hydrate concentrations [Tréhu *et al.*, 2004a]. Given that fracturing on the eastern flank of Hydrate Ridge coincides with higher  $BSR_p$  amplitudes, fracture permeability may also serve to enhance free gas concentrations at the base of the gas hydrate stability zone.

## 6. Conclusions

[41] Beneath the primary BSR ( $BSR_p$ ), we have mapped a second, weaker bottom simulating reflection ( $BSR_s$ ) across the crest of southern Hydrate Ridge with 3-D seismic reflection data.  $BSR_s$  lies 20–40 m beneath  $BSR_p$  and is observed mostly on the western flank of southern Hydrate Ridge. From observations during Leg 204,  $BSR_p$  lies at the base of the hydrate occurrence zone and is in equilibrium with pressure and temperature conditions that define the

base of hydrate stability.  $BSR_s$  is not currently the primary methane hydrate BSR. We suggest that it represents the disintegrating remnants of a BSR that existed stably for an extended period under past P-T conditions. The most likely cause for the upward migration of the BSR is changing P-T conditions within the last 18,000 years. An increase in bottom water temperatures of 1.75–2.25° and a 120 m rise in sea level shifts the BSR upward 20–40 m and fits with estimates of bottom water temperatures and sea level rise since the Last Glacial Maximum 18,000 years ago.

[42] The significance of the double BSR is that it indicates where significant amounts of gas was released from dissociated hydrate as the BSR migrated upward, and it demonstrates that the gas can stay in place for extended periods of ~5000 years. The stability of the gas is because of low permeability, and slow diffusion along the western flank of Hydrate Ridge. On the eastern flank of Hydrate Ridge, faults have formed and fracture permeability is higher. The fracture pathways contribute to disperse  $BSR_s$  faster, and direct methane released by gas hydrate dissociation migrate back into the gas hydrate stability zone to reform as hydrate. There is no evidence for escape of methane to the ocean through this process.

[43] **Acknowledgments.** We thank JGR Associate Editor William Waite, Brandon Dugan, Warren Wood, and an anonymous reviewer for helpful comments and suggestions that improved the manuscript. This research used samples and/or data provided by the Ocean Drilling Program (ODP). ODP is sponsored by the U.S. National Science Foundation (NSF) and participating countries under management of Joint Oceanographic

Institutions (JOI), Inc. This work was funded by JOI-USSSP F00161, NSF OCE-9907205, and OCE-0002487 at UTIG and OCE-9906990 and OCE-0002410 at OSU. This is UTIG contribution 1724.

## References

- Andreassen, K., J. Mienert, P. Bryn, and S. C. Singh (2000), A double gas-hydrate related bottom simulating reflector at the Norwegian continental margin, in *Gas Hydrates: Challenges for the Future*, edited by G. D. Holder and P. R. Bishnoi, *Ann. N. Y. Acad. Sci.*, 912, 126–135.
- Bangs, N. L., A. M. Tréhu, and M. Sen (2001), Mapping methane-rich fluid systems within southern Hydrate Ridge with high-resolution 3-D seismic reflection data, *Eos Trans. AGU*, 82(47), Fall Meet. Suppl., Abstract OS12B-0422.
- Crank, J. (1975), *The Mathematics of Diffusion*, Clarendon, Oxford, U.K.
- Dickens, G. R., and M. S. Quinby-Hunt (1994), Methane hydrate stability in seawater, *Geophys. Res. Lett.*, 21, 2115–2118.
- Domenico, S. N. (1976), Effect of brine-gas mixture on velocity in an unconsolidated sand reservoir, *Geophysics*, 41, 882–894.
- Foucher, J.-P., H. Nouzé, and P. Henry (2002), Observation and tentative interpretation of a double BSR on the Nankai slope, *Mar. Geol.*, 187, 161–175.
- Gorman, A. R., W. S. Holbrook, M. J. Hornbach, K. L. Hackwith, D. Lizarralde, and I. Pecher (2002), Migration of methane gas through the hydrate stability zone in a low-flux hydrate province, *Geology*, 30, 327–330.
- Hein, J. R., D. W. Scholl, J. A. Barron, M. G. Jones, and J. Miller (1978), Diagenesis of late Cenozoic diatomaceous deposits and formation of the bottom simulating reflector in southern Bering Sea, *Sedimentology*, 25, 155–181.
- Henry, P., M. Thomas, and M. B. Clennel (1999), Formation of natural gas hydrates in marine sediments: 2. Thermodynamic calculations of stability conditions in porous sediments, *J. Geophys. Res.*, 104, 23,005–23,022.
- Kennett, J. P., K. G. Cannariato, I. L. Hendy, and R. J. Behl (2003), *Methane Hydrates in Quaternary Climate Change: The Clathrate Gun Hypothesis*, 216 pp., AGU, Washington, D. C.
- Kuramoto, S., K. Tamaki, M. G. Langseth, D. C. Nobes, H. Tokuyama, K. A. Pisciotto, and A. Taira (1989), Can opal-A/opal-CT BSR be an indicator of the thermal structure of the Yamato Basin, Japan Sea?, *Proc. Ocean Drill. Program Sci. Results*, 127/128, 1145–1156.
- Levine, I. N. (1978), *Physical Chemistry*, McGraw-Hill, New York.
- Louden, K. E., and J. A. Wright (1989), Marine heat flow data: A new compilation of observations and brief review of its analysis, in *CRC Handbook of Seafloor Heat Flow*, edited by J. A. Wright and K. E. Louden, pp. 3–67, CRC Press, Boca Raton, Fla.
- Martin, J. B., M. Kastner, P. Henry, X. Le Pichon, and S. Lallement (1996), Chemical and isotopic evidence for sources of fluids in a mud volcano field seaward of the Barbados accretionary wedge, *J. Geophys. Res.*, 101, 20,325–20,345.
- Mienert, J., K. Andreassen, J. Posewang, and D. Lukas (2000), Changes of the hydrate stability zone of the Norwegian marine from glacial to interglacial times, in *Gas Hydrates: Challenges for the Future*, edited by G. D. Holder and P. R. Bishnoi, *Ann. N. Y. Acad. Sci.*, 912, 200–210.
- Mikada, H., et al. (2002), *Proceedings of the Ocean Drilling Program, Initial Reports* [CD-ROM], vol. 196, Ocean Drill. Program, College Station, Tex.
- Milkov, A. V., G. E. Claypool, Y.-J. Lee, W. Xu, G. R. Dickens, W. S. Borowski, and ODP Leg 204 Scientific Party (2003), In situ methane concentrations at Hydrate Ridge, offshore Oregon: New constraints on the global gas hydrate inventory from an active margin, *Geology*, 31, 833–836.
- Miller, J. J., M. W. Lee, and R. von Huene (1991), An analysis of a seismic reflection from the base of the gas hydrate zone, offshore Peru, *AAPG Bull.*, 75, 910–924.
- Pecher, I. A., N. Kukowski, C. R. Ranero, and R. von Huene (2000), Gas hydrates along the Peru and Middle America Trench systems, in *Natural Gas Hydrates: Occurrence, Distribution, and Detection*, *Geophys. Monogr. Ser.*, vol. 124, edited by C. K. Paull and W. P. Dillon, pp. 257–271, AGU, Washington, D. C.
- Posewang, J., and J. Mienert (1999), The enigma of double BSRs: Indicators for changes in the hydrate stability field?, *Geo Mar. Lett.*, 19, 157–163.
- Ruppel, C. (1997), Anomalous cold temperatures observed at the base of the gas hydrate stability zone on the U.S. Atlantic passive margin, *Geology*, 25, 699–702.
- Sloan, E. D. (1997), *Clathrate Hydrates of Natural Gases*, CRC Press, Boca Raton, Fla.
- Tréhu, A. M., I. Asudeh, T. M. Brocher, J. Luetgert, W. D. Mooney, J. L. Nabelek, and Y. Nakamura (1994), Crustal architecture of the Cascadia forearc, *Science*, 265, 237–243.
- Tréhu, A. M., N. L. Bangs, M. A. Arsenaault, G. Bohrmann, C. Goldfinger, J. E. Johnson, Y. Nakamura, and M. E. Torres (2002), Complex subsurface plumbing beneath southern Hydrate Ridge, Oregon continental margin, from high-resolution 3-D seismic reflection and OBS data, paper presented at Fourth International Conference on Gas Hydrates, Heat Transfer Soc. of Jpn., Yokohama, Japan.
- Tréhu, A. M., et al. (2003a) *Proceedings of the Ocean Drilling Program, Initial Reports* [CD-ROM], vol. 204, Ocean Drill. Program, College Station, Tex.
- Tréhu, A. M., D. S. Stakes, C. D. Bartlett, J. Chevallier, R. A. Duncan, S. K. Goffredi, S. M. Potter, and K. A. Salamy (2003b), Seismic and seafloor evidence for free gas, gas hydrates, and fluid seeps on the transform margin offshore Cape Mendocino, *J. Geophys. Res.*, 108(B5), 2263, doi:10.1029/2001JB001679.
- Tréhu, A. M., et al. (2004a), Three-dimensional distribution of gas hydrate beneath the seafloor: constraints from ODP Leg 204, *Earth Planet. Sci. Lett.*, 845–862.
- Tréhu, A. M., P. B. Flemings, N. L. Bangs, J. Chevallier, E. Gràcia, J. E. Johnson, C.-S. Liu, X. Liu, M. Riedel, and M. E. Torres (2004b), Feeding methane vents and gas hydrate deposits at south Hydrate Ridge, *Geophys. Res. Lett.*, 31, L23310, doi:10.1029/2004GL021286.
- Turcotte, D. L., and G. Schubert (1982), *Geodynamics, Applications of Continuum Physics to Geological Problems*, John Wiley, Hoboken, N. J.
- Ussler, W., III, and C. K. Paull (2001), Ion exclusion associated with marine gas hydrate deposits, in *Natural Gas Hydrates: Occurrence, Distribution, and Detection*, *Geophys. Monogr. Ser.*, vol. 124, edited by C. K. Paull and W. P. Dillon, pp. 41–51, AGU, Washington, D. C.
- von Huene, R., and I. A. Pecher (1999), Neotectonics and the origins of BSRs along the Peru margin, *Earth Planet. Sci. Lett.*, 166, 47–55.
- Waelbroeck, C., L. Labeyrie, E. Michel, J. C. Duplessy, J. F. McManus, K. Lambeck, E. Balbon, and M. Labracherie (2002), Sea-level and deep water temperature changes derived from benthic foraminifera isotopic records, *Quat. Sci. Rev.*, 21, 295–305.
- Westbrook, G. K., et al. (1994), *Proceedings of the Ocean Drilling Program, Initial Reports*, vol. 146, Part 1, pp. 5–14, Ocean Drill. Program, College Station, Tex.

N. L. B. Bangs, University of Texas Institute for Geophysics, 4412 Spicewood Springs Rd., Austin, TX 78759, USA. (nathan@utig.utexas.edu)

R. J. Musgrave, Department of Earth Sciences, La Trobe University, Bundoora, Victoria 3086, Australia. (r.musgrave@latrobe.edu.au)

A. M. Tréhu, College of Oceanic and Atmospheric Sciences, Oregon State University, 104 Ocean Admin Bldg, Corvallis, OR 97331-5503, USA. (trehu@oce.orst.edu)